Journal of Atmospheric and Solar-Terrestrial Physics xxx (2017) 1–8

Contents lists available at ScienceDirect

Journal of Atmospheric and Solar-Terrestrial Physics

journal homepage: www.elsevier.com/locate/jastp

Response of noctilucent cloud brightness to daily solar variations

P. Dalin [a,b,*], N. Pertsev [c], V. Perminov [c], A. Dubietis [d], A. Zadorozhny [e], M. Zalcik [f], I. McEachran [g], T. McEwan [g], K. Černis [h], J. Grønne [i], T. Taustrup [j], O. Hansen [i], H. Andersen [i], D. Melnikov [k], A. Manevich [k], V. Romejko [l], D. Lifatova [m]

[a] Swedish Institute of Space Physics, Box 812, SE-981 28 Kiruna, Sweden
[b] Space Research Institute, RAS, Profsoyuznaya St. 84/32, Moscow, 117997, Russia
[c] A. M. Obukhov Institute of Atmospheric Physics, RAS, Pyzhevskiy per., 3, Moscow, 119017, Russia
[d] Laser Research Center, Vilnius University, Saulėtekio Ave. 10, LT-10223, Vilnius, Lithuania
[e] Division for Atmospheric Research, Novosibirsk State University, Pirogova Street 2, Novosibirsk, 630090, Russia
[f] NLC CAN AM Network, #7 14130 80 Street, Edmonton, AB, T5C 1L6, Canada
[g] NLC NET, 14 Kersland Road, Glengarnock, Ayrshire, KA14 3BA Scotland, UK
[h] Institute of Theoretical Physics and Astronomy, Vilnius University, Sauletekio Ave. 3, LT-10257, Vilnius, Lithuania
[i] The Danish Association for NLC Research, Denmark
[j] The Taustrup Ovesen Cooperation (TOC) Observatory, Århus, Denmark
[k] Institute of Volcanology and Seismology, RAS, 9 Piip Boulevard, Petropavlovsk-Kamchatsky, 683006, Russia
[l] The Moscow Association for NLC Research, Kosygina St. 17, Moscow, 119334, Russia
[m] The Faculty of Physics, M.V. Lomonosov Moscow State University, 1-2, Leninskie Gory, Moscow, 119991, Russia

ARTICLE INFO

Keywords:
Noctilucent clouds
Polar mesospheric clouds
Summer mesopause
Solar activity

ABSTRACT

For the first time, long-term data sets of ground-based observations of noctilucent clouds (NLC) around the globe have been analyzed in order to investigate a response of NLC to solar UV irradiance variability on a day-to-day scale. NLC brightness has been considered versus variations of solar Lyman-alpha flux. We have found that day-to-day solar variability, whose effect is generally masked in the natural NLC variability, has a statistically significant effect when considering large statistics for more than ten years. Average increase in day-to-day solar Lyman-α flux results in average decrease in day-to-day NLC brightness that can be explained by robust physical mechanisms taking place in the summer mesosphere. Average time lags between variations of Lyman-α flux and NLC brightness are short (0–3 days), suggesting a dominant role of direct solar heating and of the dynamical mechanism compared to photodissociation of water vapor by solar Lyman-α flux. All found regularities are consistent between various ground-based NLC data sets collected at different locations around the globe and for various time intervals. Signatures of a 27-day periodicity seem to be present in the NLC brightness for individual summertime intervals; however, this oscillation cannot be unambiguously retrieved due to inevitable periods of tropospheric cloudiness.

1. Introduction

Noctilucent clouds (NLC) or the so-called night shining clouds are the highest clouds in the Earth's atmosphere formed and observed in summer time in the mesopause region between 80 and 90 km. NLC are composed of small water-ice crystals (~30–100 nm in radius) which effectively scatter sunlight, and hence these clouds are easily discernible against the twilight sky. NLC are observed from the end of May to September in the Northern Hemisphere and from the end of November to February in the Southern Hemisphere (Bronshten and Grishin, 1970; Gadsden and Schröder, 1989). NLC are also observed from space and in this case they are called Polar Mesospheric Clouds (PMC) (Thomas, 1984).

Atmospheric dynamics plays a crucial role in variability of NLC and of PMC on short- and long-term scales. Thus, turbulence, gravity and planetary waves, solar thermal and lunar gravitational tides produce significant variabilities of all basic atmospheric parameters, hence changing temporal and spatial evolution of NLC/PMC (Witt, 1962; Rapp et al., 2002; Kirkwood and Stebel, 2003; Chandran et al., 2010; Dalin et al., 2010, 2011; Pautet et al., 2011; Taylor et al., 2011; Fiedler et al., 2011; Pertsev et al., 2015; von Savigny et al., 2017). In particular, daily

* Corresponding author. Swedish Institute of Space Physics, Box 812, SE-981 28 Kiruna, Sweden.
E-mail address: pdalin@irf.se (P. Dalin).

https://doi.org/10.1016/j.jastp.2018.01.025
Received 2 November 2017; Received in revised form 15 December 2017; Accepted 23 January 2018
Available online xxxx
1364-6826/

and day-to-day temperature variations are about 6–15 K due to gravity waves (Rapp et al., 2002; Rauthe et al., 2006; Offermann et al., 2009), about 2–10 K due to traveling planetary waves (Merkel et al., 2008; Offermann et al., 2009; Dalin et al., 2011; Stevens et al., 2017), and 0.5–6 K due to solar thermal tides (Forbes, 1982a,b; Offermann et al., 2009; Fiedler et al., 2011; Stevens et al., 2017).

Besides natural atmospheric dynamics, variability of solar ultraviolet irradiance produces pronounced effects on the upper mesosphere radiative-photochemical state and to a lesser extent on the NLC/PMC radiative-photochemical-thermodynamic state (e.g., Brasseur and Solomon, 1984; Thomas et al., 2015). The solar Lyman-α flux at 121.6 nm is the primary component in the solar spectrum that drives atmospheric changes at altitudes of 70–100 km and exhibits large variability (by factor of 2) in the course of the well-known 11-year solar activity cycle (Woods and Rottman, 1997; Beig et al., 2008). Model studies (Schmidt et al., 2006; Marsh et al., 2007) as well as ground-based OH measurements (e.g., Ammosov et al., 2014; Kalicinsky et al., 2016; Perminov et al., 2017) demonstrate a positive temperature response of several degrees (1–10 K) in the mesopause region when solar activity changes from its minimum to maximum. A similar temperature (T) response of 4–5 K at 80 km altitude to solar activity was found by Hervig and Siskind (2006) using UARS HALOE satellite data. Changes in the water vapor (H_2O) concentration in the summer mesopause and above anticorrelate with solar activity mainly by Lyman-α flux-induced photodissociation of water molecules (e.g., Brasseur and Solomon, 1984; Lübken et al., 2009; Hartogh et al., 2010). Changes in T and H_2O translate into a moderate influence of the 11-year solar activity on the quasi-decadal variability in NLC/PMC characteristics. Thus, long-term ground-based NLC observations demonstrate that a significant part (20–60%) of the overall variance in the NLC occurrence frequency and brightness can be explained due to the 11-year solar variability (Dalin et al., 2006; Kirkwood et al., 2008; Dubietis et al., 2010; Pertsev et al., 2014). Satellite observations demonstrate a similar influence (30–65%) of solar activity on the total variance of the PMC extinction and albedo (brightness) in the Northern Hemisphere, depending on latitude bands and time intervals analyzed (Hervig and Siskind, 2006; DeLand et al., 2007; DeLand and Thomas, 2015).

Besides the long-term solar variability the short-term periodic perturbations in solar UV radiation occurring on a scale of 27 days (the Carrington solar rotation cycle) influence the middle atmospheric radiative-photochemical and dynamical state (Ebel et al., 1986; Hood et al., 1991; Beig et al., 2008). Tejfel (1957) was probably the first who proposed an idea that short-periodic changes in UV solar radiation can influence NLC brightness. Robert et al. (2010) were the first to demonstrate a 27-day solar signature in the NLC occurrence frequency by analyzing satellite data. Thurairajah et al. (2017) have analyzed PMC data and have found anticorrelation between variations in solar Lyman-α flux and variations in PMC ice water content, albedo and occurrence frequency. von Savigny et al. (2013) have analyzed NLC satellite observations and have found that NLC occurrence rate and albedo anomalies anticorrelate with Lyman-α flux anomalies in terms of the 27-day and the 11-year solar cycle.

In the present paper, we investigate a day-to-day response of the NLC brightness to day-to-day solar variations in the Lyman-α flux within the 27-day solar rotation cycle. Such an analysis is performed for the first time since it is based on ground-based NLC observations, carried out from different sites around the globe and for various time intervals and epochs.

2. Data source

We have analyzed daily ground-based NLC observations performed at the following sites of the Northern Hemisphere and for the following time periods:

- Scotland for 2006–2016,
- Canada for 1967–1977,
- Novosibirsk for 2004–2016,
- Moscow for 1962–2016,
- Lithuania for 1992–2016,
- Denmark for 2007–2016.

The observations have been conducted in summer time from about 20 May to 15 August. Since 2004, visual observations have been systematically supported by time-lapse digital photographic measurements in Novosibirsk and Moscow and later at other sites. The digital measurements provide continuous observations during a whole night and whole summer season with higher temporal resolution and precision compared to the visual observations. That is why the number of detected NLC displays has increased since the start of the “digital” era. At the same time, we apply the same procedure for assessment of NLC parameters both for the “digital” and “visual” observational era. In particular, the NLC brightness is visually estimated by the same procedure as described below. The total NLC number as well as the number of visual and digital NLC observations for each database is shown in Table 1. Since the Canadian NLC database contains observations made at different sites at different latitudes, we have selected only those sites which are located between 50° and 60°N in order to be consistent with NLC observations being made at midlatitudes of other databases. Details of the world-wide automated digital camera NLC network and observational techniques can be found in (Dalin et al., 2008; Dubietis et al., 2010, 2011; Zalcik et al., 2016).

As a proxy of the solar activity, daily solar Lyman-α flux data from 1962 to 2016 have been analyzed by means of satellite data obtained from the LASP Interactive Solar Irradiance Datacenter (LISIRD) and

Table 1
Sensitivity (S), along with its error (either 1.5 or 2 or 3 standard deviations), of the natural logarithm of the NLC brightness (B) to solar anomaly for various NLC databases for various time periods. The probability level of the respective S-value is shown in brackets. In the second column, the S–values are shown at time lag equal to zero day. In the third column, the maximum S-values are shown at respective average non–zero time lag (see the text). The exception is for the Moscow and Danish NLC databases, for which the maximum S-values are found at zero time lag. Statistically significant S-values (S is equal to or greater than its error) are marked in bold. The fourth column represents the coefficient of elasticity (E), i.e., the relative S-value in %/%. The fifth column yields the average lag and its statistical error range (in brackets) for the six databases (see text). The sixth column gives the number of positive (lag+), including zero, and negative (lag–) time lags determined for individual summer seasons for each database. The seventh column shows the number of visual (vis), digital (dig) as well as the total number (tot) of NLC observations for each database.

Site and time period	S [ln(B)/1 0^{11} ph cm^{-2} s^{-1}] @ lag = 0 day	S [ln(B)/1 0^{11} ph cm^{-2} s^{-1}] @ non–zero lag [day]	E (%/%)	lag and its error [days]	lag+/ lag–	vis/dig/tot
Scotland 2006–2016	**−0.27 ± 0.25** (90%)	**−0.28 ± 0.25** (90%); lag = 1	−0.04	1 (−6 +7)	7/4	0/304/304
Canada 1967–1977	**−0.19 ± 0.19** (90%)	**−0.23 ± 0.23** (95%); lag = 3	−0.02	3 (−4 +6)	9/2	969/0/969
Novosibirsk 2004–2016	**−0.32 ± 0.32** (95%)	**−0.34 ± 0.33** (95%); lag = 1	−0.05	1 (−7 +5)	9/4	0/249/249
Lithuania 1992–2016	**−0.20 ± 0.19** (90%)	**−0.29 ± 0.23** (95%); lag = 2	−0.05	2 (−1 +8)	11/14	275/258/533
Denmark 2007–2016	**−0.26 ± 0.25** (90%)		−0.04	0 (−6 +7)	4/6	0/197/197
Moscow 1962–2016	**−0.28 ± 0.28** (99%)		−0.05	0 (−4 +4)	31/20	465/350/815

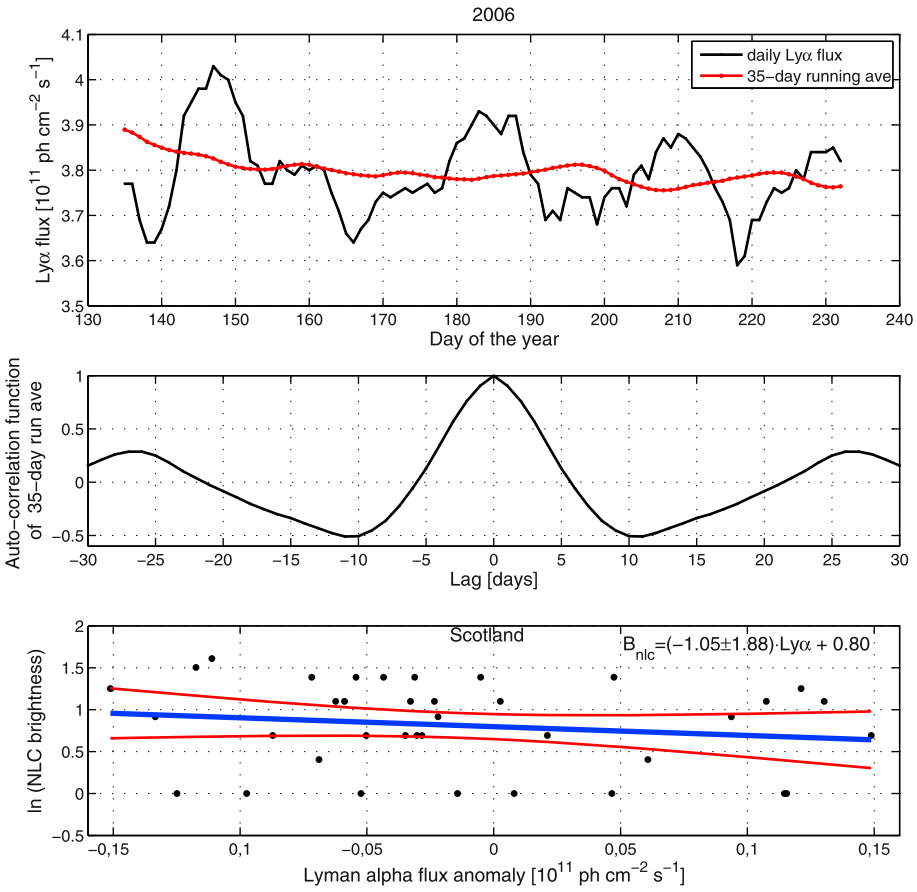

Fig. 1. The upper panel: an example of the daily solar Lyman-α irradiation data set for the summer of 2006. The black line is the daily Lyman-α time series, the red line is the smoothed Lyman-α data sets in the form of the 35-day running average. The middle panel: auto-correlation function of the 35-day running average. The lower panel: an example of the sensitivity analysis of the natural logarithm of the Scottish NLC brightness to solar anomaly for the summer of 2006. The blue line is the linear regression (sensitivity), the red lines are the 90% confidence interval. (For interpretation of the references to colour in this figure legend, the reader is referred to the Web version of this article.)

available online at: http://lasp.colorado.edu/lisird.

3. Method of analysis

For the sake of consistency with previous studies, we have analyzed daily solar Lyman-α flux data following procedures described in (Hood et al., 1991; Gruzdev et al., 2009; Robert et al., 2010; Thomas et al., 2015; Thurairajah et al., 2017). Namely, the first step is to obtain a smoothing time curve of solar Ly-α irradiance; this is done by calculating a 35-day running average over the whole time interval considered (1962–2016). These results were cross-checked by a polynomial of order 3 by the least-squares fitting for all summer months (20 May – 15 August) of this period, which provided very similar results. The second step is to calculate the difference between the original Ly-α daily data and the 35-day-smoothed curve, which is called the solar anomaly, being further considered and discussed in the paper.

The brightness of night-shining clouds is the main parameter being analyzed in the present study. The NLC brightness is visually estimated on a 5-point scale (with an increment of 0.5) as the difference between the apparent NLC brightness and the background twilight sky. The lowest value at the threshold visibility is 0.5 points and the maximum brightness is equal to 5 points (Romejko et al., 2003; Dubietis et al., 2010). In this study, we use the natural logarithm of the NLC brightness since visual brightness estimation is a logarithmic function of the light intensity due to the empiric psychophysiological Weber–Fechner law (Fechner, 1860). During the preanalysis, the logarithmic function of the NLC brightness was tested to yield a better statistical significance compared to a linear function of the NLC brightness.

In the next step, we utilize the multiple regression analysis (MRA) applied to the NLC brightness time series for each summer time data sets (intermediate step) as well as to the combined NLC databases (final step) at each site for the whole time period indicated in section 2. The MRA includes both the solar anomaly and linear time term in order to investigate a pure effect of the solar anomaly on the NLC brightness. The detailed description of the MRA technique can be found in the thematic literature (e.g., DeLand et al., 2007; Pertsev et al., 2014).

Since there can be a time lag between the solar forcing and mesospheric parameters (T, H_2O, wind circulation) response, one can expect the presence of some time lag between the solar forcing and NLC brightness as well. We investigate this important issue by introducing a time lag (in days) into the MRA. Following Thomas et al. (2015), the time lag is put positive when the NLC response follows the solar forcing. If the NLC response is ahead of the solar forcing, then the time lag is negative. By varying the time lag we search for the maximum linear regression coefficient of the solar anomaly term, fitted to all available data points for each NLC database.

Finally we have obtained the maximum average regression coefficient (slope) of the solar anomaly term, which is conventionally called "sensitivity, S" in the thematic literature (Gruzdev et al., 2009; Shapiro et al., 2012; von Savigny et al., 2013; Thomas et al., 2015; Thurairajah et al., 2017), as well as the respective average time lag for each NLC database considered (see section 2).

4. Results

An example of the Lyman-α daily irradiation data and its smoothed data sets for the summer of 2006 are presented in the upper panel of Fig. 1. The middle panel demonstrates the auto-correlation function of the 35-day running average. As one can see there exists very short periodic variations of 3–5 days in the Lyman-α flux seen on the upper panel; however when considering the 35-day running average these short periodic variations are filtered out, leaving just the main period of the solar rotation of ~27 days and, to a lesser extent, its second harmonic of 13.5-days (if its strength exceeds the strength of the main harmonic). The

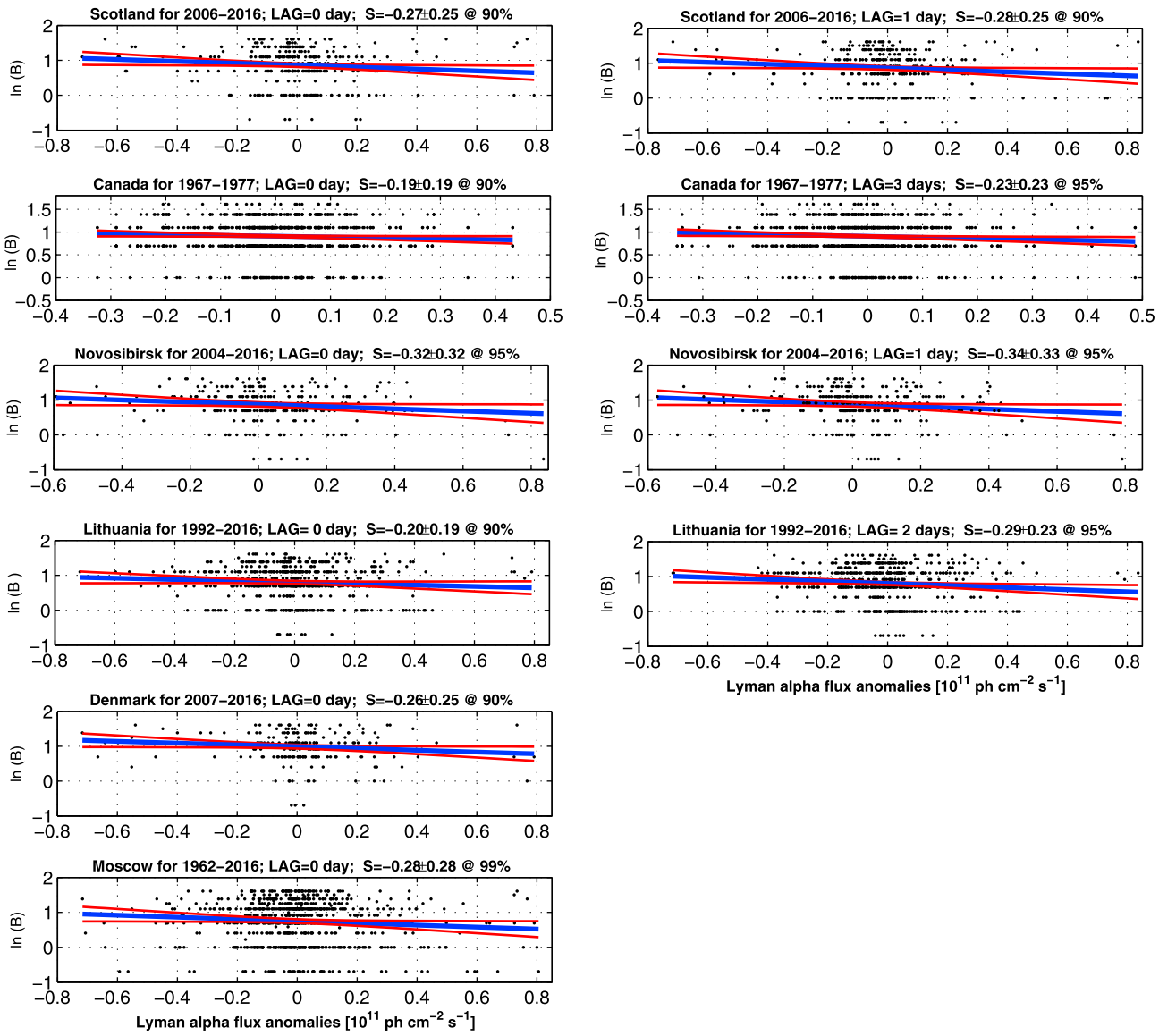

Fig. 2. The sensitivity analysis (S-value) of the natural logarithm of the NLC brightness ln(B) to solar anomaly. The left-hand side panels show average linear regression (blue line) and its error (red lines) at zero time lag for various NLC databases for various time periods. The right-hand side panels demonstrate the maximum average linear regression obtained at respective average non-zero time lags. The exception is for the Danish and Moscow NLC databases, for which the maximum S-values are found at zero time lag. (For interpretation of the references to colour in this figure legend, the reader is referred to the Web version of this article.)

lower panel of Fig. 1 illustrates an example of the sensitivity analysis for Scottish NLC brightness estimations of 2006.

By analyzing various NLC data sets for various individual summer time periods we have found different sensitivities with different signs (plus and minus) and different time lags, varying between −8 and +17 days. Note that Thurairajah et al. (2017) have also obtained negative time lags (up to −5 days) for individual summer seasons when considering CIPS and SOFIE instrument satellite data of PMC measurements. The authors have emphasized that "*However, we also get negative time lags, which could indicate the influence of non-solar processes, since it is unreasonable that the solar variability follows the PMC variability.*" It is important to note that the S-values for individual summer seasons have been found to be statistically insignificant. Such a highly variable behavior of the sensitivity for individual summer times can be due to two factors:

a) natural (dynamical) variability in the mesopause region, which plays a dominating role in the day-to-day NLC variability, masking actual time lags due to the solar forcing, yielding a wide range of S-values and time lags for an individual summer season;
b) tropospheric cloud coverage significantly masks actual NLC activity and hence actual NLC brightness estimation for an individual summer time.

Thus, the MRA result for a single year does not provide a representative/robust physical value but rather its mathematical description. That is why the MRA result should be obtained in the statistical sense based on multiple year ground-based observations in order to minimize the two aforementioned destructive interfering effects.

The MRA results for the combined NLC databases (for all analyzed summer time periods, as provided in section 2) are shown in Fig. 2 and summarized in Table 1. The left-hand side panels of Fig. 2 demonstrate the sensitivity analysis (S-values) of the natural logarithm of the NLC brightness, ln(B), to solar anomaly; average linear regression (blue line) and its error (red lines) are shown at zero time lag for various NLC databases. The right-hand side panels demonstrate the maximum average

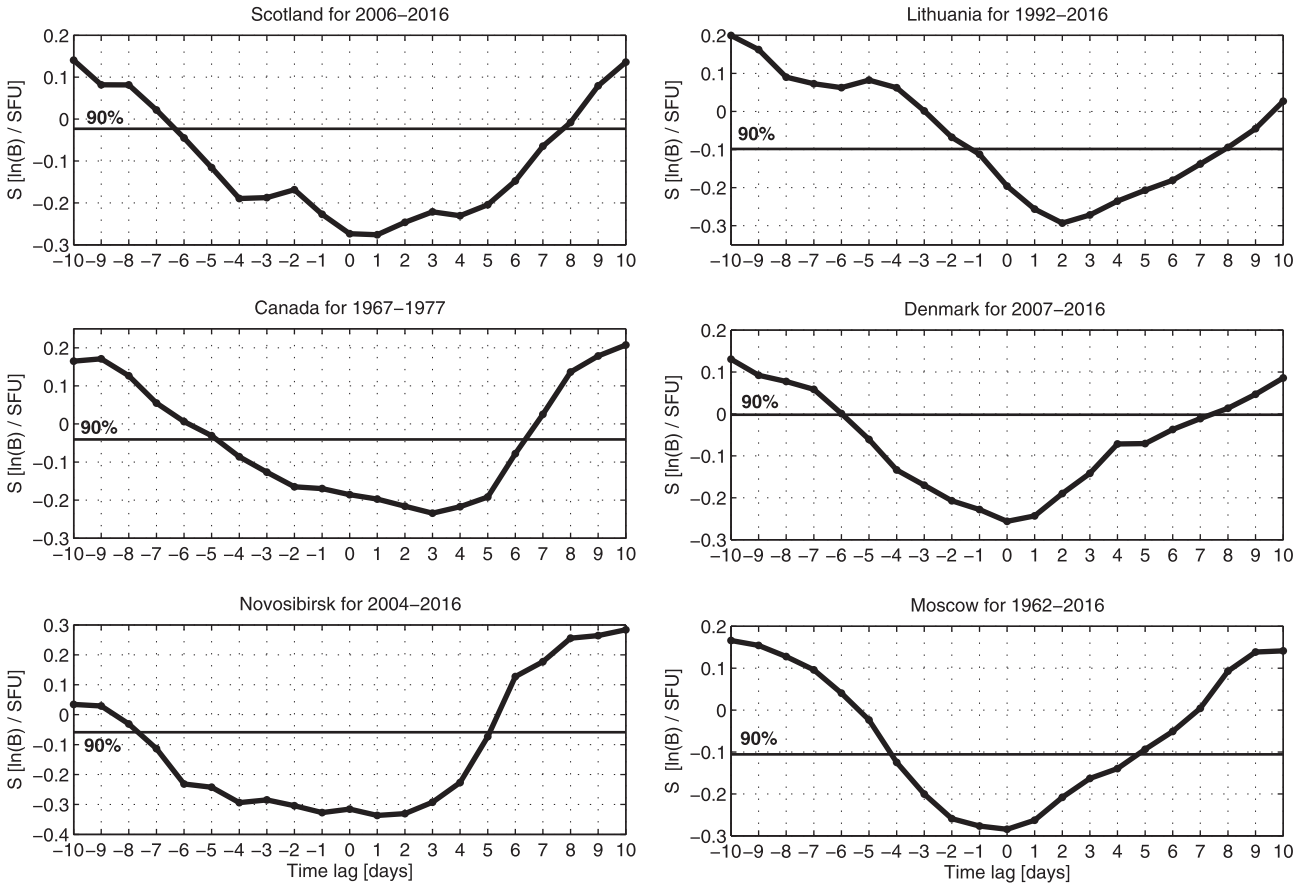

Fig. 3. The average sensitivity as a function of time lag for each NLC database. The lower limit of the 90% confidence interval, which determines the statistical significance level of the average sensitivity and the corresponding range of time lags, is shown by the solid horizontal line.

linear regression obtained at respective non-zero time lags. The exception is given for the Danish and Moscow NLC databases, for which the maximum S-values have been found at zero time lag. The following important results can be drawn by considering Fig. 2 and Table 1:

a) All NLC databases show a clear average response of the NLC brightness to the solar anomaly, i.e., the average day-to-day NLC brightness decreases with the average day-to-day increase in the solar anomaly ($S = -0.19$: -0.34 ln(B)/1 0^{11} ph cm^{-2} s^{-1}).
b) Introducing the time lag into the Lyman-α time series does improve the response of the NLC brightness to solar anomaly, i.e., the S-value is getting greater when non–zero time lag between Lyman-α and NLC time series is considered (except the Danish and Moscow NLC databases). The positive sign of the average time lags indicates a physical process: NLC response follows solar forcing.
c) All the dependences have been found to be highly statistically significant at the 90% confidence level and greater.
d) The coefficient of elasticity (relative S-value) for various NLC databases shows about the same value, suggesting that the average NLC response to the solar anomaly is almost independent of NLC time series and of observational site.

In order to estimate the statistical significance of the obtained average time lags we have plotted the average sensitivity as a function of time lag for each NLC database (Fig. 3). The error of the average lag is estimated as the range of lags for the sensitivities equal to or less than the lower limit of the 90% confidence interval shown in Fig. 3. The statistical error of the average time lag for the six databases is indicated in Table 1.

5. Discussion

It is generally considered that daily UV solar variability plays a minor role in day-to-day NLC changes. Indeed, we could not find any statistically significant influence of solar anomaly upon day-to-day NLC brightness for any individual summer season. It is rather expected since natural (dynamical) oscillations in background parameters of the summer mesopause play a major role as we have outlined in Introduction. At the same time, as shown in section 4, when NLC data are integrated for ten years and more solar forcing exhibits a statistically significant effect on day-to-day NLC brightness, i.e., average day-to-day NLC brightness decreases with average day-to-day increase in the Ly-α flux anomaly. The time lag between Lyman-α and NLC time series generally improves the average reciprocal response of the NLC brightness to the average Lyman-α forcing (except the Moscow and Danish NLC databases). We consider three main physical mechanisms lying behind these statistical results, which are currently suggested and discussed in the thematic literature (Gruzdev et al., 2009; Robert et al., 2010; Shapiro et al., 2012; von Savigny et al., 2013; Thomas et al., 2015; Thurairajah et al., 2017):

a) direct Ly-α heating/cooling of the summer mesopause due to radiation absorption by molecular oxygen;
b) photodissociation of water vapor by the Ly-α flux in the mesopause region;
c) dynamically-driven mechanism, i.e., UV radiation absorption by ozone induces changes in the stratospheric-mesospheric wind circulation, which in turn induces changes in adiabatic heating/cooling of the summer sub-polar and polar mesopause (von Savigny et al., 2013).

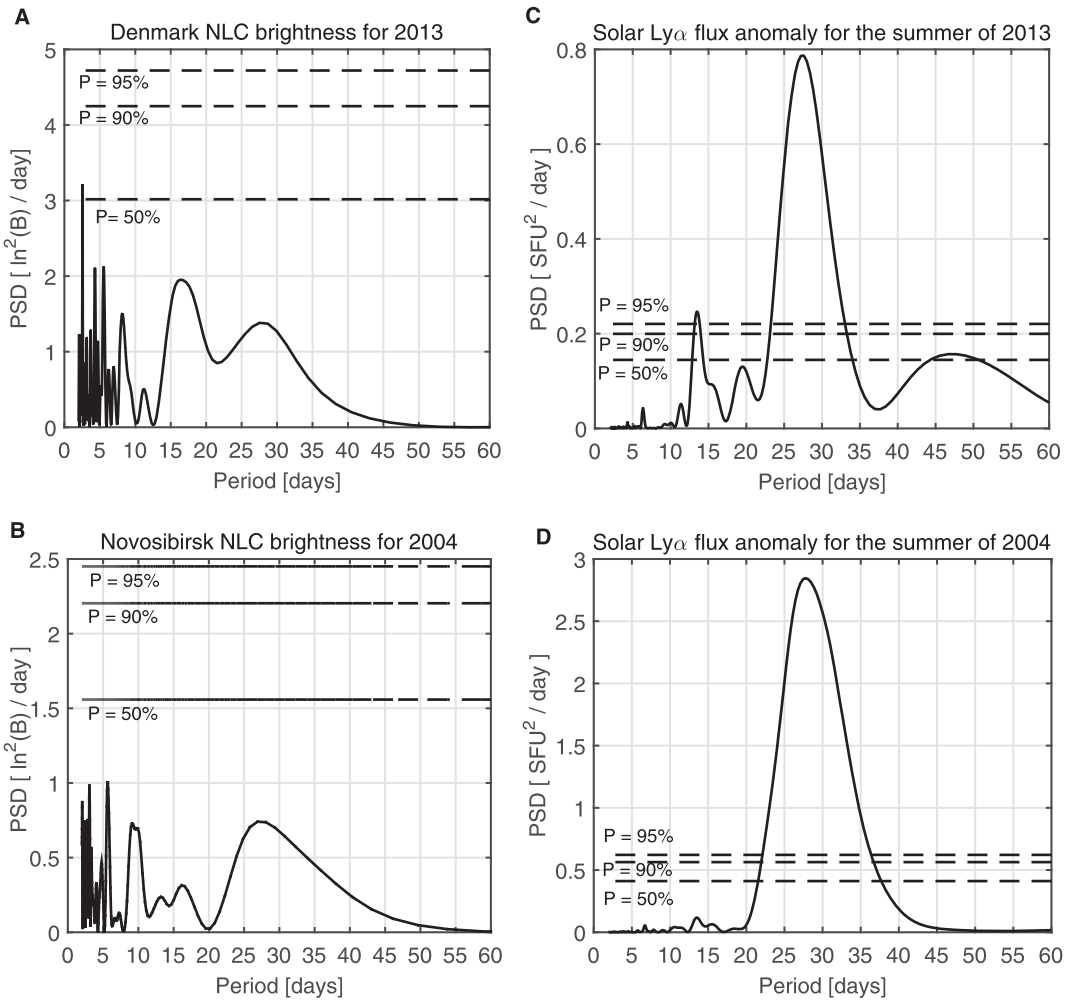

Fig. 4. Examples of the power spectrum density of the natural logarithm of NLC brightness for the Danish NLC time series for 2013 (panel A) and the Novosibirsk NLC time series for 2004 (panel B). The power spectrum density of the Lyman-α flux anomaly is for the summer of 2013 (panel C) and is for the summer of 2004 (panel D).

There can be a combination of these processes as well.

On the other hand, the established short time lags of 0–3 days may help us to identify the relevance of the above listed physical mechanisms. It is well known from theoretical studies that photochemical lifetime of water vapor in the upper mesosphere is rather long, of about 5–10 days (Nicolet, 1981; Brasseur and Solomon, 1984; Fleming et al., 1995). This can produce similar time lags between changes in the Lyman-α flux and H_2O number density (due to photolysis) in the mesopause region, which is confirmed by experimental studies (Shapiro et al., 2012), who have found a strong negative H_2O response to the solar irradiance between 78 and 90 km with time lags of 6–7 days. The authors have noticed that "*The non-zero time-lag can be attributed to the lifetime of H_2O at these heights.*" Robert et al. (2010) have also found a significant anticorrelation with a 5 day lag between H_2O and Lyman-α anomalies at 85 km in the Northern Hemisphere for the summer season of 2005. At the same time, in a number of studies (Robert et al., 2010; Thomas et al., 2015) the time lags between H_2O and Lyman-α anomalies were found to be very short (0–3 days) in the mesopause region, depending on altitude and time period analyzed. Thomas et al. (2015) have emphasized that "… *the short time lags of the water vapor (0–3 days) brings the photodissociation process into doubt.*" The authors have explained such short time lags in terms of a dynamical effect between the solar forcing and induced changes in the vertical wind in the upper mesosphere.

Using both observational and model studies, Thomas et al. (2015) have demonstrated rather short time lags (3–5 days) for the temperature sensitivity between 81 and 86 km (NLC height range), and Gruzdev et al. (2009) have modeled nearly the same temperature time lags (2–6 days) at the same height interval. By analyzing MLS temperature measurements, von Savigny et al. (2013) have found a clear correlation between the temperature and Lyman-α anomalies with a near zero time lag in the mesopause region; the temperature amplitudes were found to be 0.3–0.5 K in the course of the 27-day solar cycle. Robert et al. (2010) have demonstrated a correlation between the temperature and Lyman-α anomaly with time lags between – 5 and + 2 days, depending on time interval considered. Using SBUV and SCIAMACHY instrument satellite data, Robert et al. (2010) and von Savigny et al. (2013) have proved a significant anticorrelation between the averaged daily NLC occurrence rate/NLC brightness anomalies and averaged daily Lyman-α anomaly with near zero time lags in the course of the 27-day solar rotation. Both Robert et al. (2010) and von Savigny et al. (2013) have concluded that "… *temperature is likely the main driver affecting the variation of NLC on the 27 day time scale.*" Using CIPS satellite instrument data, Thurairajah et al. (2017) have found a significant anticorrelation between the averaged daily PMC brightness/occurrence frequency and averaged daily solar anomaly in the Northern Hemisphere with about zero time lag.

Thus, the established short (0–3 days) time lags between the NLC brightness and solar forcing suggest that the observed variations of NLC brightness are induced mainly by direct solar heating/cooling and dynamically-driven mechanism, leaving photodissociation of the water vapor as secondary. Summarizing this topic, an early assumption of Tejfel

(1957) on the influence of short-periodic changes in UV solar radiation on the NLC/PMC brightness appears to be true.

As far as a 27-day cycle in ground-based NLC observations is concerned, we have carefully analyzed every available summer season in searching for the presence of a potential 27-day periodicity in the NLC time series. We could not find any statistically significant periodicity close to 27 days in the power spectrum density (PSD) of the NLC brightness. This is rather expected since the tropospheric cloudiness significantly deteriorates such "long-term" periodicities in the NLC occurrence frequency in the course of a summer season. At the same time, we have found some signatures of the presence of the 27-day variability in NLC for particular summer seasons. In Fig. 4 we present an example of the PSD for the Danish and Novosibirsk NLC brightness for 2013 and 2004, panels A and B respectively. The PSD was calculated using the Lomb-Scargle periodogram method (Lomb, 1976; Scargle, 1982). The advantage of the Lomb-Scargle method is that it can handle non-uniformly sampled signals or data with missing samples, that is valid in the case of ground-based NLC observations. It is clearly seen that there are spectral peaks close to 27 days in the spectra, although they lack statistical significance. At the same time, strong quasi 27-day periodicity in the solar activity exists during these summer time periods (panels C and D), confirming principal possibility of the existence of the solar-induced 27-day period in the NLC data sets. When the entire period (ten years and more) of NLC observations is considered, the 27-day NLC periodicity disappears (smears out) caused by the deteriorating effect of weather conditions.

6. Conclusions

We have analyzed day-to-day observations of the NLC brightness of six NLC databases around the globe in relation to day-to-day variations in the solar Lyman-α flux. We can conclude the following:

1. Day-to-day Lyman-α variations have a minor effect on NLC brightness variations compared to other dynamical processes taking place in the summer mesopause for an individual summer season. However, when averaging over many summer seasons (ten years and more) the effect becomes rather pronounced: increase in the Lyman-α flux leads to decrease in the NLC brightness, i.e., the average negative response of the NLC brightness is observed. The effect is clearly present in all analyzed databases and is highly statistically significant (90–99%).

2. Short (0–3 days) time lags between the NLC brightness and solar forcing are established for all analyzed data sets, suggesting a prominent role of the direct solar heating of the summer mesopause due to absorption of the Lyman-α radiation by molecular oxygen and of dynamically-induced effects in the stratospheric-mesospheric wind circulation. The photodissociation of water vapor seems to play a secondary role in the average response of the NLC brightness to changes in the solar Lyman-α flux.

3. Signatures of the solar-induced 27-day variation are present in ground-based NLC observations for some individual summer seasons; however, it is extremely difficult to unambiguously retrieve this oscillation from NLC data sets contaminated by the interference effect due to tropospheric cloudiness.

Acknowledgments

The authors are grateful to all observers of noctilucent clouds around the world who contributed to the formation of the NLC databases being analyzed in the present study. We thank Takuya Sugiyama for his technical support of the NLC photo recording in Moscow for 2000-2003 and in Novosibirsk for 2000–2006. We thank two anonymous reviewers for valuable comments and suggestions which allowed us to improve the manuscript. The work was partly supported by the Russian Foundation for Basic Research under project 15-05-04975a. A copy of the paper by Tejfel (1957) can be found at the ResearchGate network. NLC ground-based data will be made available on request.

Appendix A. Supplementary data

Supplementary data related to this article can be found at https://doi.org/10.1016/j.jastp.2018.01.025.

References

Ammosov, P., Gavrilyeva, G., Ammosova, A., Koltovskoi, I., 2014. Response of the mesopause temperatures to solar activity over Yakutia in 1999–2013. Adv. Space Res. 54 (12), 2518–2524. https://doi.org/10.1016/j.asr.2014.06.007.

Beig, G., Scheer, J., Mlynczak, M.G., Keckhut, P., 2008. Overview of the temperature response in the mesosphere and lower thermosphere to solar activity. Rev. Geophys. 46 (RG3002). https://doi.org/10.1029/2007RG000236.

Brasseur, G., Solomon, S., 1984. Aeronomy of the Middle Atmosphere, second ed. D. Reidel Publishing Company, Dordrecht, Holland.

Bronshten, V.A., Grishin, N.I., 1970. Noctilucent Clouds. Nauka, Moscow.

Chandran, A., Rusch, D.W., Merkel, A.W., Palo, S.E., Thomas, G.E., Taylor, M.J., Bailey, S.M., Russell III, J.M., 2010. Polar mesospheric cloud structures observed from the cloud imaging and particle size experiment on the Aeronomy of Ice in the Mesosphere spacecraft: atmospheric gravity waves as drivers for longitudinal variability in polar mesospheric cloud occurrence. J. Geophys. Res. 115 (D13102) https://doi.org/10.1029/2009JD013185.

Dalin, P., Kirkwood, S., Andersen, H., Hansen, O., Pertsev, N., Romejko, V., 2006. Comparison of long-term Moscow and Danish NLC observations: statistical results. Ann. Geophys. 24, 2841–2849.

Dalin, P., Pertsev, N., Zadorozhny, A., Connors, M., Schofield, I., Shelton, I., Zalcik, M., McEwan, T., McEachran, I., Frandsen, S., Hansen, O., Andersen, H., Sukhodoev, V., Perminov, V., Romejko, V., 2008. Ground-based observations of noctilucent clouds with a northern hemisphere network of automated digital cameras. J. Atmos. Sol. Terr. Phys. 70, 1460–1472.

Dalin, P., Pertsev, N., Frandsen, S., Hansen, O., Andersen, H., Dubietis, A., Balciunas, R., 2010. A case study of the evolution of a Kelvin-Helmholtz wave and turbulence in noctilucent clouds. J. Atmos. Sol. Terr. Phys. 72 (14–15), 1129–1138. https://doi.org/10.1016/j.jastp.2010.06.011.

Dalin, P., Pertsev, N., Dubietis, A., Zalcik, M., Zadorozhny, A., Connors, M., Schofield, I., McEwan, T., McEachran, I., Frandsen, S., Hansen, O., Andersen, H., Sukhodoev, V., Perminov, V., Balčiunas, R., Romejko, V., 2011. A comparison between ground-based observations of noctilucent clouds and Aura satellite data. J. Atmos. Sol. Terr. Phys. 73 (14–15), 2097–2109. https://doi.org/10.1016/j.jastp.2011.01.020.

DeLand, M.T., Shettle, E.P., Thomas, G.E., Olivero, J.J., 2007. Latitude-dependent long-term variations in polar mesospheric clouds from SBUV version 3 PMC data. J. Geophys. Res. 112 (D10315) https://doi.org/10.1029/2006JD007857.

DeLand, M.T., Thomas, G.E., 2015. Updated PMC trends derived from SBUV data. J. Geophys. Res. Atmos. 120, 2140–2166. https://doi.org/10.1002/2014JD022253.

Dubietis, A., Dalin, P., Balčiūnas, R., Černis, K., 2010. Observations of noctilucent clouds from Lithuania. J. Atmos. Sol. Terr. Phys. 72, 1090–1099. https://doi.org/10.1016/j.jastp.2010.07.004.

Dubietis, A., Dalin, P., Balciunas, R., Cernis, K., Pertsev, N., Sukhodoev, V., Perminov, V., Zalcik, M., Zadorozhny, A., Connors, M., Schofield, I., McEwan, T., McEachran, I., Frandsen, S., Hansen, O., Andersen, H., Grönne, J., Melnikov, D., Manevich, A., Romejko, V., 2011. Noctilucent clouds: modern ground-based photographic observations by a digital camera network. Appl. Optic. 50 (28), F72–F79. https://doi.org/10.1364/AO.50.000F72.

Ebel, A., Dameris, M., Hass, H., Manson, A.H., Meek, C.E., 1986. Vertical change of the response to solar activity oscillations with periods around 13 and 27 days in the middle atmosphere. Ann. Geophys. 4, 271–280.

Fechner, G.T., 1860. Elemente der psychophysik, 2 volumes. Druck und Verlag von Breitkopf und Härtel (Leipzig).

Fiedler, J., Baumgarten, G., Berger, U., Hoffmann, P., Kaifler, N., Lübken, F.-J., 2011. NLC and the background atmosphere above ALOMAR. Atmos. Chem. Phys. 11, 5701–5717. https://doi.org/10.5194/acp-11-5701-2011.

Fleming, E.L., Chandra, S., Jackman, C.H., Considine, D.B., Douglass, A.R., 1995. The middle atmospheric response to short and long term solar UV variations: analysis of observations and 2D model results. J. Atmos. Sol. Terr. Phys. 57 (4), 333–365.

Forbes, J.M., 1982a. Atmospheric tides: I. Model description and results for the solar diurnal component. J. Geophys. Res. 87 (A7), 5222–5240.

Forbes, J.M., 1982b. Atmospheric tides: II. The solar and lunar semidiurnal components. J. Geophys. Res. 87 (A7), 5241–5252.

Gadsden, M., Schröder, W., 1989. Noctilucent Clouds. Springer, New York.

Gruzdev, A.N., Schmidt, H., Brasseur, G.P., 2009. The effect of the solar rotational irradiance variation on the middle and upper atmosphere calculated by a three-dimensional chemistry-climate model. Atmos. Chem. Phys. 9, 595–614.

Hartogh, P., Sonnemann, G.R., Grygalashvyly, M., Song, L., Berger, U., Lübken, F.-J., 2010. Water vapor measurements at ALOMAR over a solar cycle compared with model calculations by LIMA. J. Geophys. Res. 115 (D00I17) https://doi.org/10.1029/2009JD012364.

Hervig, M., Siskind, D., 2006. Decadal and inter-hemispheric variability in polar mesospheric clouds, water vapor, and temperature. J. Atmos. Sol. Terr. Phys. 68, 30–41.

Hood, L.L., Huang, Z., Bougher, S.W., 1991. Mesospheric effects of solar ultraviolet variations: further analysis of SME IR ozone Nimbus 7 SAMS temperature data. J. Geophys. Res. 96 (D7), 12,989–13,002.

Kalicinsky, C., Knieling, P., Koppmann, R., Offermann, D., Steinbrech, W., Wintel, J., 2016. Long-term dynamics of OH* temperatures over central Europe: trends and solar

correlations. Atmos. Chem. Phys. 16, 15033–15047. https://doi.org/10.5194/acp-16-15033-2016.

Kirkwood, S., Dalin, P., Rechou, A., 2008. Noctilucent clouds observed from the UK and Denmark – trends and variations over 43 years. Ann. Geophys. 26, 1243–1254.

Kirkwood, S., Stebel, K., 2003. Influence of planetary waves on noctilucent clouds occurrence over NW Europe. J. Geophys. Res. 108 (D8), 8440. https://doi.org/10.1029/2002JD002356.

Lomb, N.R., 1976. Least-squares frequency analysis of unequally spaced data. Astrophys. Space Sci. 39, 447–462.

Lübken, F.-J., Berger, U., Baumgarten, G., 2009. Stratospheric and solar cycle effects on long-term variability of mesospheric ice clouds. J. Reophys. Res 114 (D00I06). https://doi.org/10.1029/2009JD012377.

Marsh, D.R., Garcia, R.R., Kinnison, D.E., Boville, B.A., Sassi, F., Solomon, S.C., Matthes, K., 2007. Modeling the whole atmosphere response to solar cycle changes in radiative and geomagnetic forcing. J. Geophys. Res. 112 (D23306).

Merkel, A.W., Garcia, R.R., Bailey, S.M., Russell III, J.M., 2008. Observational studies of planetary waves in PMCs and mesospheric temperature measured by SNOE and SABER. J. Geophys. Res. 113 (D14202).

Nicolet, M., 1981. The photodissociation of water vapor in the mesosphere. J. Geophys. Res. 86 (C6), 5203–5208.

Offermann, D., Gusev, O., Donner, M., Forbes, J.M., Hagan, M., Mlynczak, M.G., Oberheide, J., Preusse, P., Schmidt, H., Russell III, J.M., 2009. Relative intensities of middle atmosphere waves. J. Geophys. Res. 114 (D06110) https://doi.org/10.1029/2008JD010662.

Pautet, P.-D., Stegman, J., Wrasse, C.M., Nielsen, K., Takahashi, H., Taylor, M.J., Hoppel, K.W., Eckermann, S.D., 2011. Analysis of gravity waves structures visible in noctilucent cloud images. J. Atmos. Sol. Terr. Phys. 73 (14–15), 2082–2090. https://doi.org/10.1016/j.jastp.2010.06.001.

Perminov, V.I., Semenov, A.I., Pertsev, N.N., Medvedeva, I.V., Dalin, P.A., Sukhodoev, V.A., 2017. Multi-year behaviour of the midnight OH* temperature according to observations at Zvenigorod over 2000-2016. Adv. Space Res. https://doi.org/10.1016/j.asr.2017.07.020.

Pertsev, N., Dalin, P., Perminov, V., 2015. Influence of semidiurnal and semimonthly lunar tides on the mesopause as observed in hydroxyl layer and noctilucent clouds characteristics. Geomagn. Aeron. 55 (6), 811–820. https://doi.org/10.1134/S0016793215060109.

Pertsev, N., Dalin, P., Perminov, V., Romejko, V., Dubietis, A., Balčiunas, R., Černis, K., Zalcik, M., 2014. Noctilucent clouds observed from the ground: sensitivity to mesospheric parameters and long-term time series. Earth Planets Space 66, 98. https://doi.org/10.1186/1880-5981-66-98.

Rapp, M., Lübken, F.-J., Müllemann, A., Thomas, G., Jensen, E., 2002. Small scale temperature variations in the vicinity of NLC: experimental and model results. J. Geophys. Res. 107 (D19), 4392,. https://doi.org/10.1029/2001JD001241.

Rauthe, M., Gerding, M., Höffner, J., Lübken, F.-J., 2006. Lidar temperature measurements of gravity waves over Kühlungsborn (54°N) from 1 to 105 km: a winter-summer comparison. J. Geophys. Res. 111 (D24108) https://doi.org/10.1029/2006JD007354.

Robert, C.E., von Savigny, C., Rahpoe, N., Bovensmann, H., Burrows, J.P., DeLand, M.T., Schwartz, M.J., 2010. First evidence of a 27 day solar signature in noctilucent cloud occurrence frequency. J. Geophys. Res. 115 (D00I12) https://doi.org/10.1029/2009JD012359.

Romejko, V.A., Dalin, P.A., Pertsev, N.N., 2003. Forty years of noctilucent cloud observations near Moscow: database and simple statistics. J. Geophys. Res. 108 (D8), 8443,. https://doi.org/10.1029/2002JD002364.

Scargle, J.D., 1982. Studies in astronomical time series analysis. II. Statistical aspects of spectral analysis of unevenly spaced data. Astrophys. J. 263, 835–853.

Schmidt, H., Brasseur, G., Charron, M., Manzini, E., Giorgetta, M.A., Fomichev, V., Kinnison, D., Marsh, D., Walters, S., 2006. The HAMMONIA chemistry climate model: sensitivity of the mesopause region to the 11-year solar cycle and CO2 doubling. J. Clim. 19, 3903–3931.

Shapiro, A.V., Rozanov, E., Shapiro, A.I., Wang, S., Egorova, T., Schmutz, W., Peter, Th, 2012. Signature of the 27-day solar rotation cycle in mesospheric OH and H2O observed by the Aura Microwave Limb Sounder. Atmos. Chem. Phys. 12, 3181–3188.

Stevens, M.H., Lieberman, R.S., Siskind, D.E., McCormack, J.P., Hervig, M.E., Englert, C.R., 2017. Periodicities of polar mesospheric clouds inferred from a meteorological analysis and forecast system. J. Geophys. Res. Atmos. 122, 4508–4527. https://doi.org/10.1002/2016JD025349.

Taylor, M.J., Pautet, P.-D., Zhao, Y., Randall, C.E., Lumpe, J., Bailey, S.M., Carstens, J., Nielsen, K., Russell III, J.M., Stegman, J., 2011. High-latitude gravity wave measurements in noctilucent clouds and polar mesospheric clouds. In: Abdu, M., Pancheva, D. (Eds.), Aeronomy of the Earth's Atmosphere and Ionosphere, vol. 2. IAGA Special Sopron Book Series, Springer, Dordrecht, pp. 93–105. https://doi.org/10.1007/978-94-007-0326-1_7.

Tejfel, V.G., 1957. Noctilucent clouds. In: Proceedings of the Astrobotanical Sector of the National Academy of Sciences of the Republic of Kazakhstan, vol. 5, pp. 59–82 (in Russian).

Thomas, G.E., 1984. Solar Mesosphere Explorer measurements of polar mesospheric clouds (noctilucent clouds). J. Atmos. Terr. Phys. 46 (9), 819–824.

Thomas, G.E., Thurairajah, B., Hervig, M.E., von Savigny, C., Snow, M., 2015. Solar-induced 27-day variations of mesospheric temperature and water vapor from the AIM SOFIE experiment: drivers of polar mesospheric cloud variability. J. Atmos. Sol. Terr. Phys. 134, 56–68. https://doi.org/10.1016/j.jastp.2015.09.015.

Thurairajah, B., Thomas, G.E., von Savigny, C., Snow, M., Hervig, M.E., Bailey, S.M., Randall, C.E., 2017. Solar-induced 27-day variations of polar mesospheric clouds from the AIM SOFIE and CIPS experiments. J. Atmos. Sol. Terr. Phys. 162, 122–135. https://doi.org/10.1016/j.jastp.2016.09.008.

von Savigny, C., Deland, M.T., Schwartz, M.J., 2017. First identification of lunar tides in satellite observations of noctilucent clouds. J. Atmos. Sol. Terr. Phys. 162, 116–121. https://doi.org/10.1016/j.jastp.2016.07.002.

von Savigny, C., Robert, C., Rahpoe, N., Winkler, H., et al., 2013. Impact of short term variability on the polar summer mesopause and noctilucent clouds. In: Lübken, F.J. (Ed.), Climate and Weather of the Sun-earth-system (CAWSES): Highlights from a Priority Program, Chapter 20. Springer Atmospheric Sciences, Springer, Dordrecht, the Netherlands, pp. 365–382.

Witt, G., 1962. Height, structure and displacements of noctilucent clouds. Tellus 14 (1), 1–18.

Woods, T.N., Rottman, G.J., 1997. Solar Lyman α irradiance measurements during two solar cycles. J. Geophys. Res. 102, 8769–8779. https://doi.org/10.1029/96JD03983.

Zalcik, M.S., Lohvinenko, T.W., Dalin, P., Denig, W.F., 2016. North American noctilucent cloud observations in 1964-77 and 1988-2014: analysis and comparisons. J. Roy. Astron. Soc. Can. 110 (1), 8–15.